Americium Organometallic Ions Produced by Laser Ablation of AmO_2 in Polyimide

John K. Gibson

Chemical and Analytical Sciences Division, Oak Ridge National Laboratory, P.O. Box 2008, Building 5505, Oak Ridge, Tennessee 37831-6375

Received: February 16, 1998; In Final Form: April 13, 1998

Laser ablation into vacuum of a dilute dispersion of AmO_2 in polyimide produced organoamericium ions of the general formula $AmC_xH_yN_z^+$. Ion masses were determined by time-of-flight mass spectrometry, and compositions were confidently assigned for most small ions ($x \leq 6$). Comparisons of product abundances with previous results for lanthanides (Ln) and lighter actinides (An) suggest that Am behaves similarly to a lanthanide element such as Tm—both produced substantial MC_2H^+ (acetylide) and MC_4H^+. In contrast, the lighter actinides, Th, U, Np, and Pu, preferentially produced the binary carbides MC_2^+ and MC_4^+. The acetylides can be regarded as ionic species comprising M^{2+} ($[M^{2+}-\{^-:C\equiv CH\}]^+$) and the carbides as comprising M^{3+} ($[M^{3+}-\{^-:C\equiv C:^-\}]^+$). Accordingly, the MC_2H^+ vs MC_2^+ abundances generally correlated with the ionization energies from M^{2+} to M^{3+} (IE[M^{2+}]). In addition to the carbide/hydrocarbide complex ions, Am^+-hydroxide, -cyanide, -cyanate, and -nitrile ions were produced in abundances generally consistent with IE[Am^+] and IE[Am^{2+}]. Both $AmCN^+$ and AmC_2H^+ comprise nominally divalent Am^{2+}, but the relative abundance of the cyanide (vs acetylide) species was greater for Am than for the preceding An, suggesting a greater degree of ionicity in the Am complexes. Larger $AmC_xH_yN_z^+$ were identified for x up to ∼12, with compositions consistent with the ionic bonding model used to represent the smaller Am^+-R. The formation and possible structures of the larger species are considered with regard to the neutrals produced during ablation of polyimide. In addition, substantial amounts of directly ablated fullerene ions (and neutrals), $C_{50}^+-C_{\geq 125}^+$, were produced under favorable ablation conditions. An anomalously intense peak corresponding to C_{110}^+ is considered to probably comprise a contribution from the metallofullerene of similar mass, Am^+-C_{90}. On the basis of the divalent character of Am, this species could be represented as $Am^{2+}-C_{90}^-$, although the present results provide do not indicate whether such a species should be regarded as an exohedral or endohedral metallofullerene. This work extended the production of labile gas-phase organoactinide complexes to the first transplutonium element Am—this technique is applicable to highly radioactive elements not amenable to conventional methods. The results revealed the divalent character of Am not evident for the preceding An. The low-valent σ-bonded organometallics identified in the gas phase are difficult to isolate for the lanthanide and transuranium actinide elements, but polymer ablation into vacuum accesses transient/metastable species by supplying highly reactive hydrocarbon radicals to a free metal center.

Introduction

A laser ablation-mass spectrometry (LA-MS) technique was previously developed to elucidate comparative organometallic chemistries of lanthanide (Ln) and actinide (An) metal ions, M^+, with the ultimate goal of application to the scarce and highly radioactive transuranium elements, which are not readily investigated by conventional condensed-phase methods. In this approach, designated *m*etal−*p*olymer *co**a*blation (MPCA), a dispersion of a metal compound (e.g., AmO_2) in a polymer (e.g., polyimide, PI), is ablated into vacuum using a pulsed laser, and the directly ablated product ions are determined by reflectron time-of-flight mass spectrometry (RTOF-MS). The compositions and abundances of the organometallic complex ions, M^+-R, reveal comprehensible distinctions in organometallic chemistry across the Ln and An series. The initial application of MPCA was to several Ln and the light An, Th, and U[1]; subsequently, the first two transuranium actinides, Np and Pu, were similarly studied.[2]

Gas-phase M^+ + hydrocarbon (L) reactions typically produce primarily M^+-L^* by elimination of H_2 or a closed-shell hydrocarbon.[3,4] In contrast, PI ablation produces abundant fragment radicals, R,[5] such as C_n, C_nH_x (x odd), and CN,[6] as well as closed-shell ("L") species such as alkynes and nitriles.[7] On the basis of thermodynamic considerations, it is expected that the more reactive open-shell R should preferentially combine with coablated M^+ to produce σ-bonded M^+-R complexes; MPCA thereby produces labile organometallic species that may not be observed in conventional gas-phase reactions carried out under conditions of low-energy ion−molecule collisons. The M^+ can form single or multiple σ-type bonds of varying degree of ionicity to one or more unsaturated radical sites of ablated R. The abundances and structures of most neutral R ablated from PI are largely indeterminate, but previous results have demonstrated that the relative abundances of specific M^+-R consistently correlate with distinctive M^+ chemistries and elementary parameters such as the third ionization energy, IE-[$M^{2+} \rightarrow M^{3+}$].

By way of general background in this field, previous studies have determined metallic elements in polymers by laser ablation sampling, but subsequent excitation using inductively coupled plasmas obliterated the chemical speciation of the ablated material.[8] Metal-containing cluster ions have been produced

S1089-5639(98)01145-1 CCC: $15.00
Published on Web 05/20/1998

by direct laser ablation of nonpolymer mixtures—for example, $W_nC_m^+$ from W + graphite.[9] The present MPCA technique advances this latter methodology by generating more complex, multielement ions and providing clear correlations between speciation and distinctions between metal ion chemistries within the 4f and 5f series.

The few transplutonium organoactinide compounds that have been isolated are highly ionic, with the An bonded to one or more cyclopentadienylide anions, $C_5H_5^-$ (Cp^-), or substituted Cp^- ligands.[10] It is generally considered[10] that the degree of covalency in organoactinide bonding decreases across the series until fully lanthanide-like ionic behavior is obtained around Bk (due to the contraction/stabilization of the 5f electrons upon proceeding across the An series). The ability to prepare novel gas-phase organometallics with distinctive metal-dependent abundances by MPCA should better elucidate changes in organoactinide bonding across the actinide series. The primary goal of the present study was to extend MPCA to the first transplutonium element, Am. Such studies are particularly significant because the experimental challenges in studying organometallic chemistry of the scarce and highly radiotoxic transplutonium elements by conventional means are daunting and this is a distinctive region of the actinide series where the transition to quasi-lanthanide-like character is anticipated, i.e., essentially fully localized, low-energy f electrons.

To illuminate processes by which M^+-R are produced in MPCA, metal-free ablated ions and neutrals were also identified. Polymer fragment ions were established from the relatively low-mass (i.e., $<^{243}Am^+$) ion peaks. It was additionally possible to identify some of the primary small ablated *neutrals*, L, by electron impact ionization (EII) of the slow, residual portion of the ablation plume. The observed Am^+-R complexes are presumed to form by combination, in the dense nascent ablation plume, of Am^+ with one or more neutral polymer fragments R.

It is known that laser ablation of polyimide can produce substantial amounts of fullerenes,[11] suggesting the potential for preparing metallofullerenes by coablation of a metal (oxide) and polyimide. In the present MPCA experiments, conditions were varied in an attempt to optimize fullerene production and the potential for detecting Am^+-fullerene complexes. Preliminary evidence is presented for the first Am−fullerene complex.

Experimental Section

The instrument and experimental procedures were as described previously,[1,2,4,12] and only key features are summarized here. The target was prepared from a powder dispersion of 3.7 mg (0.014 mmol) of $^{243}AmO_2$ (ORNL archival sample, >99% Am-243) in 18.4 mg (1.08 mmol of carbon) of the PI, poly-{*N*,*N*′-(1,4-phenylene)-3,3′,4,4′-benzophenonetetracarboxylic imide/amic acid, $[-C_{23}H_{10}O_5N_2-]_n$ (Aldrich no. 18464-0; note that this PI differs slightly in composition and significantly in structure from the DuPont Kapton PI more commonly studied but is the same PI as used in our previous MPCA studies[1,2]). The target was prepared by compressing the Am + PI mixture into a 3 mm diameter disk using a small manual pellet press (Parr); the ^{243}Am target preparation and all subsequent handling were performed in α-containment gloveboxes in the Transuranium Research Laboratory at ORNL. The Am-243, produced in the high-flux isotope reactor at ORNL, α-decays with a half-life of 7370 y and is generally preferred over the more plentiful Am-241 isotope, which has a half-life of only 433 y.

Ablation was by a XeCl excimer laser ($\lambda = 308$ nm) with a target irradiance of $\sim$l0^8 W cm^{-2} ($\sim$0.5 mm^2 irradiated area)[1] or, in a few experiments, by a pulsed coumarin-503 (C503) dye laser ($\lambda \approx 500$ nm) with a target irradiance of $\sim 10^7$ W cm^{-2} ($\sim$10 mm^2 irradiated area).[12] Ablated positive ions propagating orthogonal to both the target surface and the RTOF-MS flight axis were injected into the −2 kV flight tube by a +200 V repeller pulse after a time delay, t_d, following the laser pulse. The distance from the target to the $\sim$6 mm^2 cross-sectional cylindrical volume of ions from the expanding ablation plume injected into the mass spectrometer was $\sim$3 cm so that by variation of t_d, it was possible to sample ions of different velocities (i.e., kinetic energies). The source region of the RTOF-MS incorporated a standard EII capability for analyzing ambient gases. Limited efficacy of EII of ablated neutrals was attributed to space charging by the glut of directly ablated ions; accordingly, useful EII spectra (170 V ionizing electrons) of ablated neutrals could only be obtained after long t_d (e.g., $\gtrsim$100 μs), by which time most ablated ions had dissipated. In the mass region of the mass spectra where the metal−ligand complexes appear, the resolution was sufficient to clearly discriminate species such as $^{243}Am^+-C_4$ and $^{243}Am^+-C_4H$ ($m/\Delta m > 600$). In the much higher mass fullerene region, a somewhat lower resolution ($m/\Delta m \approx 500$) limited the ability to discriminate species that might have resulted from attachment/incorporation of Am^+ to/into fullerenes, as discussed below. No metastable decomposition, which might have assisted in assigning ion structures, was discerned on the $\sim$100 μs time scale of the present experiments.

Results and Discussion

Low-Mass Species Produced by Ablation of AmO_2 + Polyimide. A 308 nm ablation spectrum of directly ablated PI fragment ions from 56 to 240 Da is shown in Figure 1 (above 240 Da the PI fragment ions are obscured by $^{243}Am^+-R$ species). The spectrum in Figure 1 was obtained using $t_d = 35$ μs, but the *relative* abundances did not vary appreciably upon changing t_d. For all spectra, the absolute ion intensity scales are given in millivolts—the quantity measured during the experiments—to allow direct comparisons of absolute intensities between spectra. The spectrum in Figure 1 was obtained with the EI ionizer on, but essentially, no change in the shown peaks was discernible with it switched off. However, lower-mass peaks at 17 Da (OH^+), 18 Da (H_2O^+), and 28 Da (CO^+) diminished with the EI ionizer off, indicating substantial ablated H_2O and CO (these peaks were significantly more intense than those due to residual contamination in the vacuum chamber); smaller decreases at 26 Da (CN^+) and 27 Da (HCN^+) were attributed to ablation of HCN (and possibly CN).

The complex mass spectrum in Figure 1 indicated extensive fragmentation/recombination in the ablation plume, with no indication of substantial retention of the main structural units of the PI target. As suggested by the parenthetical composition assignments shown for some of the more intense peaks in Figure 1, it is likely that the spectrum is dominated by hydrocarbon ions. Using deuterated PI, Brenna et al.[13] established that there is minimal N incorporation into such cluster ions produced under conditions similar to those employed here. The appearance of a series of comparably intense peaks at unit mass separation is furthermore consistent with primary attribution to $C_mH_x^+$, $C_mH_{x+1}^+$, $C_mH_{x+2}^+$, etc. Excimer laser ablation of PI under these conditions can be represented as a quasi-thermal pyrolysis followed by ablation of residual hydrogenated graphitic material.[14] Thermal pyrolysis of PI eliminates most of the O and N constituents as CO, CO_2, H_2O, and HCN.[15] The ions directly ablated from PI can be compared with those prepared by reaction of C_m^+ (ablated from graphite) with H_2; the incorporation of

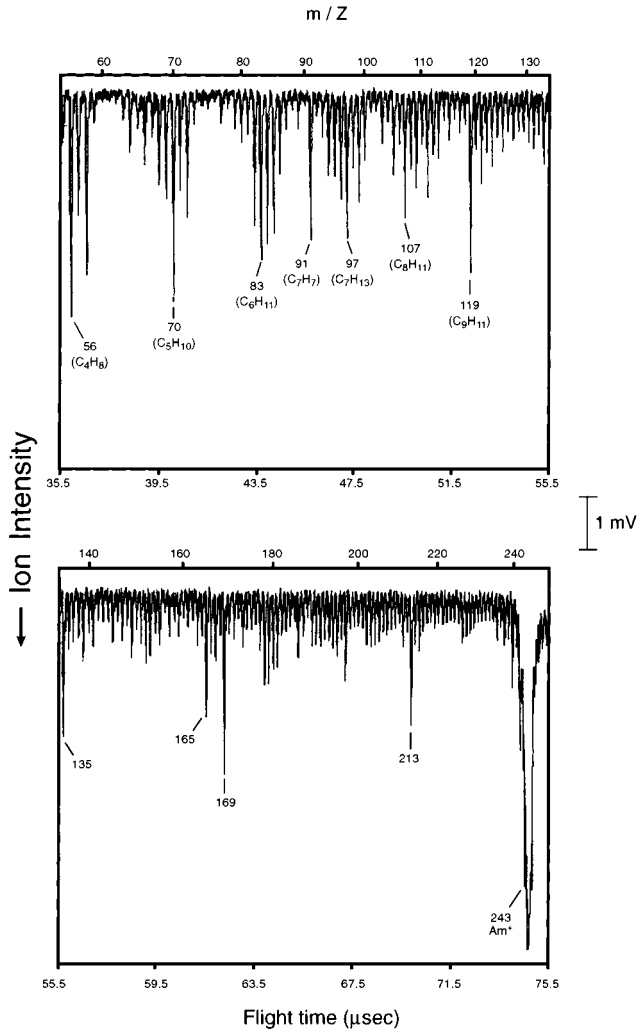

Figure 1. Mass spectrum for the Am−PI target: $\lambda = 308$ nm; $t_d =$ 35 ms; EI on. The only peaks that significantly diminished with EI off were those corresponding to OH^+, H_2O^+, and CO^+.

hydrogen in the $C_mH_x^+$ is expected to favor linear/branched (vs cyclic) structures for these ions.[16] Although there was a near continuum in the appearance of "$C_mH_x^+$," some peaks were notably more intense than others. The importance of some apparently even-*x* $C_mH_x^+$ such as "$C_4H_8^+$" and "$C_5H_{10}^+$" seems to conflict with the abundant odd-*x* ions such as "$C_6H_{11}^+$," "$C_7H_7^+$", and "$C_9H_{11}^+$" on which the electron deficiency can reside at an unsaturated C site. The observed $C_mH_x^+$ ions may largely correspond to branched hydrocarbons with a particularly stable carbocationic site at a tertiary carbon. The PI mass spectrum is intriguing but only allows speculation regarding ion formation mechanisms, compositions (e.g., possible O and/or N incorporation), and structures. It is uncertain whether the observed organometallic complex ions discussed below, $\{Am-R\}^+$, were produced primarily by association of Am^+ with neutral R or by association of neutral Am with R^+ ions. However, the great abundance of Am^+ (Figure 1) and the absence of substantial amounts of R^+, which appeared as important $\{Am-R\}^+$ constituents (e.g., the dearth of $R^+ = C_6H^+$ in Figure 1), indicate primarily the former association process: $Am^+ + R$. Accordingly, it is presumed to be ablated neutral R that combine with coablated Am^+ to produce most of the observed organometallic complexes and the directly ablated PI fragment ions R^+ are of somewhat ancillary interest.

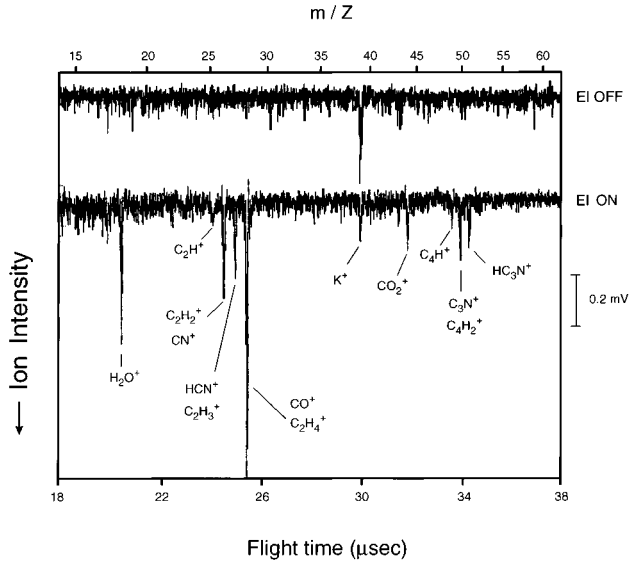

Figure 2. Mass spectra for the Am−PI target, $\lambda = 308$ nm; $t_d = 110$ μs: (top) EI off; (bottom) EI on. The only significant peak at higher mass was $^{243}Am^+$ (intensity of ~0.2 mV with EI off or on).

To further elucidate the possible mechanisms by which the observed Am^+-R were produced, experiments were performed in an attempt to determine the important ablated neutral PI fragments, R, with which coablated Am^+ could combine. Presumably owing to space-charging by the glut of directly ablated ions present in the RTOF-MS ion source at the short t_d (~35 ms) for which Am^+-R products were abundant, simultaneous EII of coablated neutrals was inefficient, as noted above in the discussion of Figure 1. However, when t_d was increased to >100 μs, the ion concentration in the source region had evidently diminished to an extent that EII spectra of ablated neutrals could be obtained; such a spectrum (for $t_d = 110$ μs) is shown in Figure 2. Above 60 Da, only a small 243 Da peak attributed to the slow component of ablated Am^+ was evident, both with EII on and off. In Figure 2, the only peak that appeared with the EII off, at 39 Da, was assigned to directly ablated K^+—potassium is a ubiquitous and easily ionized impurity. By comparison of the EII spectrum in Figure 2 with those in the NIST database,[17] it is concluded that the primary ablated slow, closed-shell neutrals were CO, CO_2, H_2O, C_2H_2, HCN, and HC_3N (HC≡C−C≡N); the possibility of some C_2H_4 (producing $C_2H_4^+$) cannot be excluded. Obviously, the PI structure was highly fragmented under XeCl laser ablation, with no evidence for intact cyclic structural units. The species sampled at long t_d represent the slow fraction of the expanding ablation plume, which were presumably formed under lower energy conditions and do not necessarily represent the important neutrals present where the Am^+-R were formed; specifically, radical species were likely produced under higher-energy conditions earlier in the plume development and dissipated more quickly, rendering them undetectable by EII at long t_d. The presence of slow, nonradical species such as hydrogen cyanide, acetylene, and HC≡C−C≡N suggests that corresponding radicals such as $^{\bullet}CN$, $^{\bullet}C_2H$, and $^{\bullet}C_3N$ were present earlier, in the dense and energetic portion of the plume.

Americium Complex Ions. Typical results for 308 nm ablation of the Am−PI target are shown in Figure 3, with the main complex ion peaks indicated. Because C_2H_2 is essentially isobaric with CN (26 Da) and because M-{26 Da} peaks were prevalent in the initial PI studies,[1] subsequent experiments were previously carried out using Ln_2O_3 + polystyrene, a nitrogen-free polymer matrix.[2] The absence of the Ln^+-{26 Da} peaks

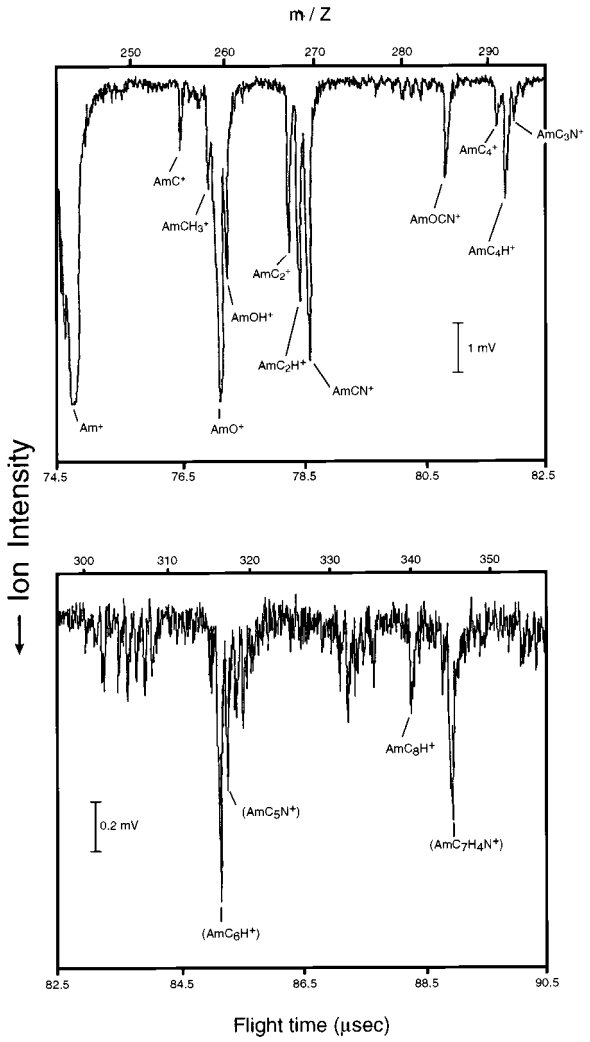

Figure 3. Mass spectrum for the Am−PI target: $\lambda = 308$ nm; $t_d = 50$ μs. Other peaks at higher mass were Am[118]$^+$ (0.3 mV) and Am[146]$^+$ (0.5 mV). Among the possible assignments are N≡C−(C_6H_4)−O^- for the mass 118 ligand and N≡C−CH_2−(C_6H_4)−CH_2−O^- or $^-$C≡C−[C≡C−]$_4$−C≡N for the mass 146 ligand.

using polystyrene indicated primary attribution of the 26 Da ligand complexes to M^+-CN rather than $M^+-C_2H_2$.[2] From generalization of the polystyrene results, some heavier ion peaks from PI were attributed to nitriles, M^+-C_mN, rather than dihydrides, $M^+-C_{m+1}H_2$, e.g., R = C_3N, not C_4H_2, and R = C_5N, not C_6H_2. These assignments were substantiated by the absence of an $Am^+-C_mH_x$ continuum in the mass spectrum. The use of deuterated polyimide would have differentiated the CN and C_2H_2 ligands, as well as other isobaric ligands such as those noted above. However, it was concluded that obtaining deuterated polyimide was not feasible under the constraints of the project within which these studies were performed. Experiments with AmO_2 + polystyrene would presumably have a better defined the degree of incorporation of N into the ligands but would have substantially contaminated the ablation chamber with highly radioactive ^{243}Am. The AnO_2 + polymer ablation experiments disperse appreciable amounts of the actinide, and this effect has been found to be particularly extreme with polystyrene from which ion yields are smaller than from PI. To minimize contamination of the instrument, the Ln_2O_3 + polystyrene results were extrapolated to Am.

The primary Am^+-R species, shown in the top portion of Figure 3, correspond to those observed under comparable conditions for Ln^+ and lighter An^+; it is the widely disparate relative abundances of these ions that reflect the differing metal ion chemistries. The Am^+ peak is off-scale in Figure 3, and the abundance of AmO^+ relative to Am^+ is minor compared to the preceding AnO^+; this accords with the relatively small dissociation energy ($D = D_0°$) of AmO[18] (e.g., D[AmO] ≈ 550 kJ mol^{-1} vs D[UO] = 774 kJ mol^{-1}).

TABLE 1: An and Ln Ion Energetics[a]

	IE[M^{2+}][b]	ground M^+ [c]	"divalent" M^+ [d]	ΔE(G/II)[e]
U	1927	$5f^3 7s^2$	$5f^3 6d^1 7s^1$	3
Np	1995	$5f^4 7d^1 7s^1$	(ground)	0
Pu	2101	$5f^6 7s^1$	$5f^5 6d^1 7s^1$	104
Am	2159	$5f^7 7s^1$	$5f^6 6d^1 7s^1$	245
Ce	1949	$4f^1 5d^2$	(ground)	0
Tm	2285	$4f^{13} 6s^1$	$4f^{12} 5d^1 6s^1$	199

[a] Energies in kJ mol^{-1}. [b] IE[$M^{2+} \rightarrow M^{3+}$]. From ref 19 ($An^{2+}$) and ref 20 ($Ln^{2+}$). [c] M^+ ground electronic configurations outside the closed-shell core, [Rn] for An and [Xe] for Ln, from ref 21 (An^+) and ref 20 (Ln^+). [d] Lowest "divalent" configuration with two non-f valence electrons, from ref 21 (An^+) or ref 20 (Ln^+). [e] Promotion energy from the ground to "divalent" M^+ configuration.

A few particularly pertinent qualitative comparisons between the typical abundances of key characteristic An^+-R complexes for U, Np, Pu, Ce, and Tm from previous studies,[1,2] and the results for Am obtained in the present study under comparable conditions are as follows:

$$UC_2^+ \gg UC_2H^+ \approx UCN^+$$

$$NpC_2^+ > NpC_2H^+ \approx NpCN^+$$

$$PuC_2^+ \approx PuC_2H^+ \approx PuCN^+$$

$$AmC_2^+ < AmC_2H^+ < AmCN^+ \quad \text{(Figure 3)}$$

$$CeC_2^+ \gg CeC_2H^+ > CeCN^+$$

$$TmC_2^+ \ll TmC_2H^+ < TmCN^+$$

It should be noted that a significant contribution to the "$AmCN^+$" peak from $AmC_2H_2^+$ is feasible, despite the indications to the contrary from the Ln_2O_3 + polystyrene experiments. By use of a rudimentary ionic bonding model, these three types of organometallic complexes can be represented as $M^{3+}-\{:C\equiv C:\}^{2-}$ (carbide), $M^{2+}-\{:C\equiv CH\}^-$ (acetylide), and $M^{2+}-\{:C\equiv N\}^-$ (cyanide). Accordingly, their relative abundances should correlate with the $M^{2+} \rightarrow M^{3+}$ ionization energies (IE[M^{2+}]), which differ appreciably for the studied An, from 1927 kJ mol^{-1} for U^{2+} to 2159 kJ mol^{-1} for Am^{2+} (Table 1). In contrast, the $M^+ \rightarrow M^{2+}$ ionization energies vary by only ~30 kJ mol^{-1} among U, Np, Pu, and Am[19] so that the facility of formation of $An^{2+}-R^-$ complexes should be comparable for each. Accordingly, the distinction between these An is anticipated in the propensity to further oxidize to form species that correspond to $An^{3+}-R^{2-}$. This effect has been demonstrated for the lanthanide elements, since the comparison of Ce and Tm included above exemplifies IE[Tm^{2+}] is 336 kJ mol^{-1} greater than IE[Ce^{2+}] (Table 1), which is manifested in the much greater affinity of Ce^+ for C_2 (to give "$Ce^{3+}-C_2^{2-}$").

The bonding in LnC_2 is apparently similar to that in LnO,[22] and the degree of ionicity in Ln−O and Ln^+-O is indeterminate;[23] the above rudimentary IE interpretation of the observed abundances must be somewhat of a simplification. Included in Table 1 are the energies required to promote a 4f/5f electron

TABLE 2: Ligand Electron Affinities[a]

	EA		EA		EA
C	121(1)	C_2	315(1)	CN	372(1)
C_3	192(1)	C_4	374(1)	NCO	348(1)
C_5	274(1)	C_6	403(1)	C_3N	424(20)
C_7	324(2)	C_8	422(1)	C_2H	282(4)
C_9	355(1)	C_{10}[b]	212(10)	C_3H	179(3)
C_{11}	377(1)	C_{60}[b]	256(1)	OH	176(1)
				CH_3	19(10)

[a] From NIST ref 17 in kJ mol^{-1}. Uncertainties are in parentheses. [b] C_{10} is cyclic and C_{60} is a fullerene. All other C_n are linear.

in ground-state Ln^+/An^+ to a 5d/6d valence orbital. This quantity can be designated $\Delta E[(M^+)^G \rightarrow (M^+)^{II}]$ (abbreviated ΔE[G/II]) because it is the energy required to prepare a ground M^+ to a configuration capable of contributing two non-f valence electrons to covalent bonding. It has been established from gas-phase organometallic experiments that the 4f/5f electrons of the Ln/An are ineffective at forming covalent (σ-type) organometallic bonds required for C−H activation (via a $C-M^+-H$ intermediate)[24] so that such promotion can be presumed to be a requisite for covalent bond formation. The ΔE[G/II] and IE[M^{2+}] included in Table 1 exemplify the observation that these quantities generally parallel one another for the f elements. Fully covalent $M^+{=}O$ would be presumed to require contribution of two non-f valence bonding electrons by the M^+ constituent, and the hypothetical fully covalent $D[M^+{=}O]$ (and $D[M^+{=}C_2]$) would be expected to approximately inversely correlate with both the ΔE[G/II] and the parallel IE[M^{2+}]. Consequently, the semiquantitative MPCA abundance comparisons do not definitively reveal the degree of ionicity in the organometallic complexes and the pure IE model is invoked somewhat arbitrarily—the actual bonding situation is undoubtedly somewhere between ionic and covalent and might be represented by resonance structures such as $M^{2+}-\{:C{\equiv}CH\}^- \leftrightarrow M^+-C{\equiv}CH$. It should be noted that the significantly smaller relative abundance of NpC_2^+ compared with that of UC_2^+ suggests appreciable ionicity because ΔE[G/II] values are essentially the same for Np^+ and U^+ (both $\Delta E \approx 0$), whereas IE[Np^{2+}] is significantly larger than IE[U^{2+}]. This is an important instance where the correlation between IE[M^{2+}] and ΔE[G/II] is poor and additional insights into the substantially ionic nature of the bonding can be inferred.

A central new result of the present experiments was the clearly discrepant behavior of Am^+ compared with that of the preceding An^+ with regard to the abundances of the small orgnaoactinide complex ions specified in the above comparisons. In particular, the relative yield of AmC_2^+ was substantially smaller than those of UC_2^+, NpC_2^+, and PuC_2^+. Rather, the "divalent" complexes AmC_2H^+ and $AmCN^+$ were preferentially produced. This result accords with the greater IE[An^{2+}] and ΔE[G/II] for Am relative to that of the preceding An. The distinctive preference of Am to form divalent organometallic complexes in the gas phase is also manifested in its inorganic chemistry in that Am is unique among the An through Bk in its ability (under extreme conditions) to form a few solid divalent compounds, such as $AmCl_2$.[25]

Whereas U, Np, and Pu each produced roughly comparable amounts of AnC_2H^+ and $AnCN^+$, the yield of $AmCN^+$ was distinctly greater than that of AmC_2H^+. Some ligand electron affinities (EA) are given in Table 2 where it is seen that EA[CN] is very large, greatly exceeding EA[C_2H]. On the basis of these EAs and the greater electron-withdrawing effect of the N in −CN compared with the 2′-C in −CCH, it is expected that the bonding in M^+-CN should be more ionic than in M^+-C_2H. Thus, the particularly large abundance of Am^+-CN suggests that Am^+-R bonding is more ionic than that for the lighter An^+-R. This accords with the trend across the An series toward increasing Ln-like behavior; Ln organometallic chemistry is dominated by ionic ligands, including acetylides $C{\equiv}CR^-$.[26] The light actinides, notably U, exhibit a greater proclivity to form σ-bonded An−C organometallics.[27]

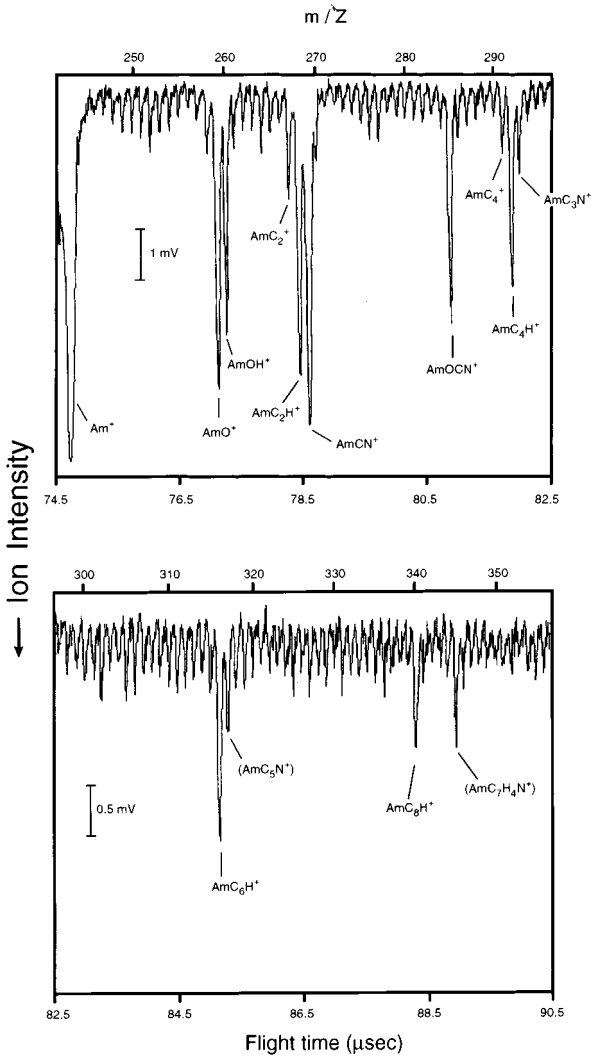

Figure 4. Mass spectrum for the Am−PI target: $\lambda = 488$ nm; $t_d = 35$ μs.

The abundances of Am^+-R for larger R are consistent with the above characterization of the apparently abrupt transition from "early actinide" to quasi-lanthanide behavior in proceeding from U/Np/Pu to Am. Most notably, the AnC_4^+, AnC_6^+, and AnC_8^+ species were significant products for the light An whereas AmC_4H^+, AmC_6H^+, and AmC_8H^+ dominated over the corresponding binary AmC_m^+. Without specification of structural configurations or the degree of covalency, these carbides can be represented as polyynes $An^{3+}-\{:C{\equiv}C-C{\equiv}C:\}^{2-}$, $Am^{2+}-\{:C{\equiv}C-C{\equiv}C-H\}^-$, etc. The preference for Am to form divalent complexes is again apparent. Theoretical results for small LaC_n clusters[28] suggest that the AnC_n^+ clusters probably exhibit a metallocyclic-type structure with the An^+ situated in the concave cavity produced by a bent C_n chain. In contrast, the Am^{2+} acetylides are presumably quasi-linear, with η^1-coordination at the unsaturated terminal carbon.

The mass spectrum shown in Figure 4 was obtained using the C503 dye laser at 488 nm, employing significantly lower

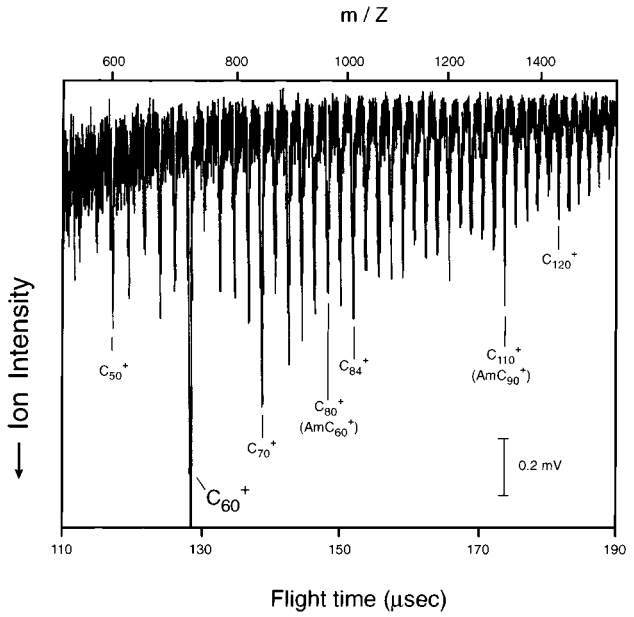

Figure 5. Fullerene portion of the mass spectrum in Figure 4.

irradiance over a larger area compared with that for the Figure 3 spectrum. It is apparent that the primary mass spectral features remained qualitatively unchanged in comparison with the results from 308 nm experiments. The somewhat greater resolution obtained for the 488 nm spectrum appears to reveal an underlying continuum of M, M + 1, M + 2, etc. peaks. However, the intense $AnC_mH_n^+$ ($m \lesssim 10$; $n \lesssim m$) carbohydride peak manifolds seen with Np and Pu are not evident for Am. This provides further evidence for the particular preference for Am^+ to combine with ablated R to form highly ionic η^1−:C$^-$ bonds. The peaks assigned in Figures 3 and 4 as AmC_3N^+ and AmC_5N^+ can be regarded as η^1-complexes of divalent Am with polyyene nitrile radicals: Am^{2+}−{:C≡C−C≡N}$^-$ and Am^{2+}−{:C≡C−C≡C−C≡N}$^-$.

Fullerenes. Under conditions where the use of EII had minimal effect on the PI fragment R^+ abundances or the Am^+−R abundances (e.g., Figure 1) it was found that use of EII greatly enhanced the intensities of the fullerene peaks (C_{2n}), indicating that neutral C_{2n} were ejected from the target with velocities comparable to those of the lighter polyimide fragment ions. The spectrum shown in Figure 5 (EII off) was among those most abundant in directly ablated fullerene ions. This spectrum was obtained using the C-503 dye laser at relatively low irradiance, and the production of abundant fullerenes under such conditions is consistent with laser ablation results obtained elsewhere employing other target substrate materials.[29]

The mass resolution for the small cluster ions was sufficient to discriminate Am−$C_mH_x^+$ from Am−$C_mH_{x+1}^+$, but the resolution in the 1000 Da region where fullerenes appear was insufficient to differentiate the potential ^{243}Am (243 Da) and $^{12}C_{20}$ (240 Da) constituents. The relatively poor resolution in the high-mass fullerene spectra was exacerbated by significant intensities of ^{13}C-containing C_{2n}^+, which results in peaks broadened toward the high-mass side of the monoisotopic $^{12}C_{2n}^+$. For example, the natural abundance of ^{13}C (1.11%) results in the following statistical isotopomeric distribution for C_{80}: 40.9% $^{12}C_{80}$; 36.8% $^{12}C_{79}{}^{13}C$; 16.3% $^{12}C_{78}{}^{13}C_2$; 4.8% $^{12}C_{77}{}^{13}C_3$, the last of which is essentially isobaric with $^{243}Am^{12}C_{60}$ (963.01 vs 963.06 Da). As a result of the limited mass resolution and the significant contribution from ^{13}C-containing isotopomers, it was not practical to ascertain Am−C_{60}^+ or other americium fullerenes by identification of discrete Am^+−C_{2n} peaks. The alternative prospect for perceiving such species was the appearance of anomalously intense (i.e., "magic number") peaks, which might indicate formation of substantial amounts of metallofullerenes. In Figure 5, as in other fullerene spectra, the standard magic number fullerenes, particularly C_{60}^+ and C_{70}^+, are obvious. The peak corresponding to C_{110}^+ appears to be anomalously intense; this ion is essentially isobaric with Am^+−C_{90}. An enhanced stability (i.e., enhanced intensity) for C_{110}^+ from PI ablation under UV laser ablation might be inferred from earlier studies.[11] To ascertain the potential contribution of Am^+−C_{90} to the "C_{110}^+" peak, a comparable experiment was carried out using 460 nm irradiation (coumarin-460 dye laser) on the Pu−PI target employed in earlier studies.[2] With this latter target, the results for the distinctively abundant small fullerenes (e.g., C_{60}^+, C_{70}^+, C_{84}^+) were comparable to those for the Am−PI target, but no enhanced intensity was apparent at or near "C_{110}^+". Rather, a nearly monotonic decrease in C_{2n}^+ peak intensities was evident beyond C_{84}^+. Again, owing to the limited mass resolution, formation of substantial $^{242}Pu^+$−C_{90} would have similarly manifested as an enhanced intensity at "C_{110}^+." This direct comparison between results for the Am−PI and Pu−PI targets supports the interpretation of a contribution to the "C_{110}^+" peak in Figure 5 from Am^+−C_{90}. The reflectron time-of-flight mass spectrometer is capable of achieving a mass resolution of >1000 ($m/\Delta m$) under EII conditions, but the resolution deteriorates for the laser ablation sampling conditions currently employed. Within the constraints imposed by performing instrumental modifications to the ion source region in a transuranic-contaminated glovebox, attempts will be made to improve the mass resolution for polymer ablation, which would facilitate definitive identification of Am^+−C_{90}.

The stability of a Am^{2+}−C_{90}^- complex relative to other Am^{2+}−C_{2n}^- can be assessed by reference to the comparative EAs of the fullerenes—EA values for C_{60}, C_{90}, and small C_n clusters are given in Table 2. On the basis of the measurements of Boltalina, et al.,[31] it is apparent that the EA of fullerenes generally increases with the size of the C_{2n} cage. Although only a lower limit was established for EA[C_{90}], the value is clearly substantially greater than EA[C_{60}] (Table 2)—it may be that EA[C_{90}] is anomalously large. The results of the present experiments leave indeterminate whether the postulated Am^+−C_{90} species should be represented as an exohedral metal carbide complex or as an endohedral metallofullerene. The endohedral species would presumably be stabilized by electrostatic interaction of the encapsulated Am^{2+} with the surrounding C_{90}^- shell but would require either growth of the fullerene cage around Am^+ or insertion of Am^+ into a formed C_{90} cage. It should finally be noted that an alternative explanation of the "C_{110}^+" peak would be Am^+−C_{70}−Am, with two Am atoms exohedral and/or endohedral to C_{70}. However, this species would have a mass 6 Da greater than that of $^{12}C_{110}^+$ and 3 Da greater than that of $^{12}C_{107}{}^{13}C_3$, and it is likely that some broadening/splitting of the "C_{110}^+" peak toward higher mass would be discernible for this greater mass separation.

The postulated Am^+−C_{90} would apparently be a unique f-element metallofullerene because the largest fullerene cage for which f-element fullerenes are typically produced are C_{82}, e.g., Sm@C_{82} [30] (Sm is chemically quite similar to Am). However, these conventional metallofullerenes were produced by incorporation of a neutral M into the fullerene cage, with the metal donating either two (e.g., Sm) or three (e.g., La) electrons. In contrast, Am^+−C_{90} resulting from MPCA is presumed to form by association (or insertion) of ablated Am^+

with C_{90}, giving $Am^{2+}-C_{90}^-$. As with the smaller $\{Am-R\}^+$, the possible formation mechanism $Am + C_{90}^+ \rightarrow \{Am-C_{90}\}^+$ is considered less likely on the basis of the absence of an especially large abundance of C_{90}^+ in the naked fullerene ion spectrum. The postulated $Am^{2+}-C_{90}^-$ would represent a unique type of f-element metallofullerene, with only one electron being donated by a preionized +1 metal ion to the fullerene cage. An additional distinction between the An^{n+} and homologous Ln^{n+} ions is the larger ionic radii of the former. This difference should favor incorporation of An ions into larger fullerene cages, such as C_{90}.

Conclusions

The primary goal of this investigation was to enhance the fundamental understanding of the organometallic chemistry of Am, which is highly radioactive and accordingly difficult or impractical to study by conventional experimental techniques. The novel gas-phase technique, MPCA, employs reactions between coablated metal ions and polymer radical fragments, thereby readily accessing highly exoergic $\{M^+ + R\}$ coalescence reactions. The basis for elucidating organoamericium bonding was primarily by comparison with other f-element organometallic complex ions produced under similar MPCA conditions. An intriguing example of condensed-phase Ln acetylide chemistry is the bridged species $\{Cp^-\}_2-\{Sm^{3+}\}-\{:C\equiv C:\}^{2-}-\{Sm^{3+}\}-\{Cp^-\}_2$.[32] As is typical in condensed-phase organolanthanide chemistry, this species comprises trivalent Ln^{3+}. A characteristic of gas-phase studies is the relative ease of accessing low-valent (unsaturated) species. This ability allows investigation of novel aspects of comparative f-element chemistries. For example, it can be rather challenging to prepare divalent Am compounds in the condensed phase, but divalent Am organometallics were the primary species produced by MPCA. It is most significant that the dominance of divalent Am complexes by MPCA distinctly contrasts with the appreciable formation of trivalent complexes for the preceding An. An ancillary interest in studying high-energy organometallic species such as those created by MPCA is that gas-phase acetylides, dicarbides, and their +1 ions, e.g., $MgCCH^+$, may be important metal-containing constituents of the interstellar medium.[33]

Attempts were made to identify the ablated PI species that might combine with the coablated Am^+ to form the observed Am^+-R complexes. Although abundant ablated PI fragment ions could be identified simultaneously with the Am^+-R complexes, the glut of ions in the ion source region rendered the conventional EII capability ineffective. It was only possible to identify a few primary closed-shell ablated neutrals, which were emitted with sufficiently low energies that they remained in the source region after most of the directly ablated ions had dissipated. The compositions of these stable molecules are consistent with the neutral cyanide, radical nitriles, acetylides, and carbides, which were presumed to be present in the early stages of the ablation process when the Am^+-R were formed. The formation of primarily M^+-R rather than M^+-L complexes is consistent with available metal ion thermochemistry data,[33] despite that the number of available $D[M^+-R]$ values are limited (reflecting the greater difficulty in producing and examining gaseous M^+-R complexes by conventional techniques). By comparison of the bonding between V^+ and C_2H_x, for example, $D[V^+-C_2] = 524$ kJ mol^{-1}, $D[V^+-C_2H] = 491$ kJ mol^{-1}, and $D[V^+-C_2H_2] = 205$ kJ mol^{-1}. Metal ion−cyanide bond energies are especially sparse, but the following estimates (theory) for Al^+ are illuminating: $D[Al^+-CN] \approx 122$ kJ mol^{-1}; $D[Al^+-C_2H_2] \approx 63$ kJ mol^{-1}.[34] It is apparent why the M^+-{26 Da} peaks should be due to M^+-CN rather than $M^+-C_2H_2$.

The particularly abundant peak at "C_{110}^+" in the Am−PI spectrum was absent in a Pu−PI spectrum obtained under similar conditions. A plausible explanation for this observation is the formation of $Am^{2+}-C_{90}^-$, an exohedral or endohedral metallofullerene complex. The formation of this distinctive species could be attributed to the combination of Am^+ with neutral C_{90}. The potential ability to produce substantial amounts of fullerenes under particular polyimide ablation conditions suggests pursuing this approach using other actinide isotopes that provide sufficient mass separation from the pure C_{2n}^+ that definitive mass spectrometric identification of actinofullerenes should be possible. For example, the 5 Da mass separation between $^{248}Cm^+-C_{60}$ and $^{12}C_{77}{}^{13}C_3$ should be discernible. Furthermore, relatively small IE[Cm^{2+}] (2043 kJ mol^{-1})[19] and ΔE[G/II] for Cm^+ (48 kJ mol^{-1})[21] are expected to promote formation of trivalent $Cm^{3+}-R^{2-}$ complexes and could additionally advance the synthesis of the more conventional type of exohedral $Cm^{3+}-C_{2n}{}^{2-}$ or endohedral $Cm^{3+}@C_{2n}{}^{2-}$ (e.g., $2n = 60$) metallofullerenes.

Acknowledgment. This work was sponsored by the Division of Chemical Sciences, Office of Basic Energy Sciences, U.S. Department of Energy, under Contract DE-AC0596OR22464 at Oak Ridge National Laboratory with Lockheed Martin Energy Research Corp. The ^{243}Am used in this study was supplied by the Division of Chemical Sciences, Office of Basic Energy Sciences, U.S. Department of Energy through the transplutonium element production facilities located at the Oak Ridge National Laboratory.

References and Notes

(1) Gibson, J. K. *J. Vac. Sci. Technol. A* **1997**, *15*, 2107−2118.
(2) Gibson, J. K. *J. Alloys Compd.*, in press.
(3) Cornehl, H. H.; Heinemann, C.; Schroder, D.; Schwarz, H. *Organometallics* **1995**, *14*, 992−999.
(4) Gibson, J. K. *J. Phys. Chem.* **1996**, *100*, 15688−15694.
(5) The symbols "L", "L*", etc. designate closed-shell ligands; "R", "R*", etc. designate radicals.
(6) Kokai, F.; Kakudate, Y.; Togashi, H.; Koga, Y.; Fujiwara, S. *Appl. Phys. A* **1995**, *60*, 31−34.
(7) Lazare, S.; Guan, W.; Drilhole, D. *Appl. Surf. Sci.* **1996**, *96*−*98*, 605−610.
(8) Hemmerlin, M.; Mermet, J. M. *Spectochim. Acta B* **1996**, *51*, 579−589.
(9) Ross, M. M.; O'Keefe, A.; Baronavski, A. P. In *Physics and Chemistry of Small Clusters*; Jena, P., Rao, B. K., Khanna, S. N., Eds.; Plenum: New York, 1987; pp 323−328.
(10) Marks, T. J.; Streitwieser, A., Jr. In *The Chemistry of the Actinide Elements*, 2nd ed.; Katz, J. J., Seaborg, G. T., Morss, L. R., Eds.; Chapman and Hall: New York, 1986; Vol. 2, pp 1547−1587.
(11) Creasy, W. R.; Brenna, J. T. *Chem. Phys.* **1988**, *126*, 453−468.
(12) Gibson, J. K. *Anal. Chem.* **1997**, *69*, 111−117.
(13) Brenna, J. T.; Creasy, W. R.; Volksen, W. *Chem. Phys. Lett.* **1989**, *163*, 499−502.
(14) Ball, Z.; Csete, M.; Ignacz, F.; Racz, B.; Szabo, G.; Sauerbrey, R. *Appl. Phys. A* **1995**, *61*, 575−578.
(15) Jakab, E.; Till, F.; Szekeley, T.; Kozhabekhov, S. S.; Zhubanov, B. A. *J. Anal. Appl. Pyrolysis* **1992**, *23*, 229−243.
(16) Lee, S.; Gotts, N.; von Helden, G.; Bowers, M. T. *J. Phys. Chem. A* **1997**, *101*, 2096−2102.
(17) Mallard, W. G.; Linstrom, P. J., Eds. Ion Energetics Data. In *NIST Standard Reference Database Number 69*; National Institute of Standards and Technology: Gaithersburg, MD, 1997 (http://webbook.nist.gov).
(18) Haire, R. G. *J. Alloys Compd.* **1994**, *213/214*, 185−190.
(19) Morss, L. R. In *The Chemistry of the Actinide Elements*, 2nd ed.; Katz, J. J., Seaborg, G. T., Morss, L. R., Eds.; Chapman and Hall: New York, 1986; Vol. 2, pp 1278−1360.
(20) Martin, W. C.; Zalubas, R.; Hagan, L. *Atomic Energy Levels-The Rare Earth Elements*; NSRDS-NBS 60; National Bureau of Standards (NIST): Washington, DC, 1978.

(21) Fred, M. S.; Blaise, J. In *The Chemistry of the Actinide Elements*, 2nd ed.; Katz, J. J., Seaborg, G. T., Morss, L. R., Eds.; Chapman and Hall: New York, 1986; Vol. 2, pp 1196−1234.
(22) Chandrasekharaiah, M. S.; Gingerich, K. A., In *Thermodynamic Properties of Gaseous Species*; Gschneidner, K. A., Jr., Eyring, L., Eds.; Elsevier: New York, 1987; Vol. 12, pp 409−431.
(23) Ackermann, R. J.; Rauh, E. G.; Thorn, R. J. *J. Chem. Phys.* **1976**, *65*, 1027−1031.
(24) (a) Cornehl, H. H.; Heinemann, C.; Schroder, D.; Schwarz, H. *Organometallics* **1995**, *14*, 992−999. (b) Gibson, J. K. *J. Am. Chem. Soc*. **1998**, *120*, 2633−2640.
(25) Katz, J. J.; Morss, L. R.; Seaborg, G. T. In *The Chemistry of the Actinide Elements*, 2nd ed.; Katz, J. J., Seaborg, G. T., Morss, L. R., Eds.; Chapman and Hall: New York, 1986; Vol. 2, pp 1121−1195.
(26) Heeres, H. J.; Nijhoff, J.; Teuben, J. H. *Organometallics* **1993**, *12*, 2609−2617.
(27) Marks, T. J. In *The Chemistry of the Actinide Elements*, 2nd ed.; Katz, J. J., Seaborg, G. T., Morss, L. R., Eds.; Chapman and Hall: New York, 1986; Vol. 2, pp 1588−1587.
(28) Ayuela, A.; Seifert, G.; Schmidt, R. *Z. Phys. D* **1997**, *41*, 69−72.
(29) Rose, H. R.; Dance, I. G.; Fisher, K. J.; Smith, D. R.; Willett, G. D.; Wilson, M. A. *J. Chem. Soc., Chem. Commun.* **1993**, 1361−1363.
(30) Moro, L.; Ruoff, R. S.; Becker, C. H.; Lorents, D. C.; Malhotra, R. *J. Phys. Chem.* **1993**, *97*, 6801−6805.
(31) Boltalina, O. V.; Sidorov, L. N.; Borshchevsky, A. Ya.; Sukhanova, E. V.; Skokan, E. V. *Rapid Commun. Mass Spectrom.* **1993**, *7*, 1009−1011.
(32) Evans, W. J.; Rabe, G. W.; Ziller, J. W. *J. Organomet. Chem.* **1994**, *483*, 21−25.
(33) Woon, D. E. *Astrophys. J.* **1996**, *456*, 602−610.
(34) Freiser, B. S., Ed., *Organometallic Ion Chemistry*; Kluwer: Dordrecht, 1996; pp 284−322.